Khan, M. A. H., Lyons, K., Chhantyal-Pun, R., McGillen, M. R., Caravan, R. L., Taatjes, C. A., ... Shallcross, D. E. (2018). Investigating the Tropospheric Chemistry of Acetic Acid Using the Global 3-D Chemistry Transport Model, STOCHEM-CRI. *Journal of Geophysical Research: Atmospheres*, *123*(11), 6267-6281. https://doi.org/10.1029/2018JD028529

Journal of Geophysical Research: Atmospheres

RESEARCH ARTICLE
10.1029/2018JD028529

Investigating the Tropospheric Chemistry of Acetic Acid Using the Global 3-D Chemistry Transport Model, STOCHEM-CRI

M. Anwar H. Khan[1], Kyle Lyons[1], Rabi Chhantyal-Pun[1], Max R. McGillen[1], Rebecca L. Caravan[2], Craig A. Taatjes[2], Andrew J. Orr-Ewing[1], Carl J. Percival[3], and Dudley E. Shallcross[1]

[1]School of Chemistry, University of Bristol, Bristol, UK, [2]Combustion Research Facility, Sandia National Laboratories, Livermore, CA, USA, [3]Jet Propulsion Laboratory, California Institute of Technology, Pasadena, CA, USA

Key Points:
- The CH_3COOH concentration hot spots are found in the tropics with highest mixing ratios of 1.6 ppb seen in South America
- The secondary production from the ocean can be a significant source of CH_3COOH over the oceans
- The reaction of CH_3COOH with Criegee intermediates exceeds 60% of the total chemical loss of CH_3COOH in the Amazon rainforest areas

Supporting Information:
- Supporting Information S1

Correspondence to:
D. E. Shallcross,
d.e.shallcross@bristol.ac.uk

Citation:
Khan, M. A. H., Lyons, K., Chhantyal-Pun, R., McGillen, M. R., Caravan, R. L., Taatjes, C. A., et al. (2018). Investigating the tropospheric chemistry of acetic acid using the global 3-D chemistry transport model, STOCHEM-CRI. *Journal of Geophysical Research: Atmospheres*, *123*. https://doi.org/10.1029/2018JD028529

Received 2 MAR 2018
Accepted 18 MAY 2018
Accepted article online 27 MAY 2018

Abstract Acetic acid (CH_3COOH) is one of the most abundant carboxylic acids in the troposphere. In the study, the tropospheric chemistry of CH_3COOH is investigated using the 3-D global chemistry transport model, STOCHEM-CRI. The highest mixing ratios of surface CH_3COOH are found in the tropics by as much as 1.6 ppb in South America. The model predicts the seasonality of CH_3COOH reasonably well and correlates with some surface and flight measurement sites, but the model drastically underpredicts levels in urban and midlatitudinal regions. The possible reasons for the underprediction are discussed. The simulations show that the lifetime and global burden of CH_3COOH are 1.6–1.8 days and 0.45–0.61 Tg, respectively. The reactions of the peroxyacetyl radical (CH_3CO_3) with the hydroperoxyl radical (HO_2) and other organic peroxy radicals (RO_2) are found to be the principal sources of tropospheric CH_3COOH in the model, but the model-measurement discrepancies suggest the possible unknown or underestimated sources which can contribute large fractions of the CH_3COOH burden. The major sinks of CH_3COOH in the troposphere are wet deposition, dry deposition, and OH loss. However, the reaction of CH_3COOH with Criegee intermediates is proposed to be a potentially significant chemical loss process of tropospheric CH_3COOH that has not been previously accounted for in global modeling studies. Inclusion of this loss process reduces the tropospheric CH_3COOH level significantly which can give even larger discrepancies between model and measurement data, suggesting that the emissions inventory and the chemical production sources of CH_3COOH are underpredicted even more so in current global models.

1. Introduction

Acetic acid (CH_3COOH) plays a significant role in the acidity of precipitation and cloud water in the troposphere (Galloway et al., 1982; Keene et al., 1995; Khare et al., 1999; Vet et al., 2014; Zhang et al., 2011). Keene and Galloway (1986), and Andreae et al. (1988) proposed that carboxylic acids could account for as much as 80–90% of precipitation acidity in remote regions of the world. Because of the characteristic hygroscopic nature of the carboxylic acids and their ability to act as cloud condensation nuclei (Yu, 2000), they are responsible for absorbing and dispersing solar radiation, thus altering the global thermal balance.

The well-constrained sources of CH_3COOH in the atmosphere include anthropogenic, vegetation, soil, and biomass burning which can contribute to the atmospheric burden of CH_3COOH (Paulot et al., 2011). While direct anthropogenic emissions are a significant source of CH_3COOH in industrialized areas, biogenic emissions are of greater importance in remote regions (Chebbi & Carlier, 1996). Soil emissions may be an important source of CH_3COOH, especially in environments with low levels of terrestrial vegetation (Enders et al., 1992; Sanhueza & Andreae, 1991). Owing to the extensive array of factors that impact the emission of CH_3COOH from soil, that is, soil composition, vegetation cover, temperature, humidity, and other meteorological parameters, local and global fluxes remain poorly catalogued. While direct vegetative emissions of CH_3COOH do occur (Schäfer et al., 1992; Talbot et al., 1990, 1995) and contribute to its atmospheric presence, it is indirect production following photochemical conversion of precursor volatile hydrocarbons (e.g., isoprene) that represents the main source of atmospheric CH_3COOH and leads to the seasonal pattern of atmospheric concentrations (Paulot et al., 2011). The unconstrained sources include motor exhaust emissions (Grosjean, 1989, 1992; Kawamura et al., 1985; Zervas et al., 2001), atmospheric transformation of enols (Archibald et al., 2007), and aqueous phase oxidation of methylglyoxal (Carlton et al., 2006; Lim et al., 2005) may contribute to the global emission sources of CH_3COOH. A recent study (Keene et al., 2015)

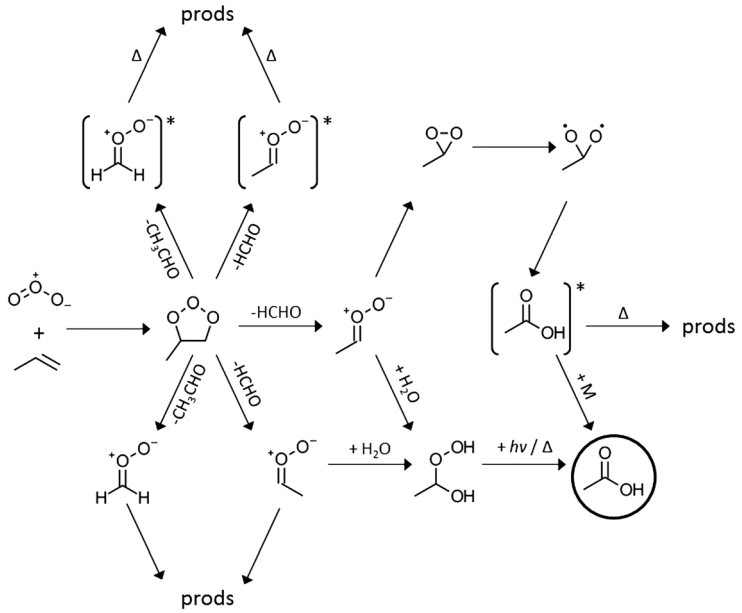

Scheme 1. Criegee reaction scheme and the formation of CH_3COOH.

suggests that the photochemical degradation of particulate organic matter associated with both marine aerosols and biomass burning may be a source of CH_3COOH. The relatively small spatial variability in concentration and wet-deposition flux of carboxylic acids over broad geographic regions in their study suggests a fairly uniform marine source strength globally.

The key chemical production channel is thought to be the oxidation of olefins producing CH_3COOH via the Criegee intermediate (Calvert & Stockwell, 1983). The Criegee reaction that produces CH_3COOH can be written as shown in Scheme 1.

Scheme 1 depicts the ozone-initiated oxidation of propene, although it is noted that trans-2-butenes and other alkenes that form the acetaldehyde oxide moiety will have analogous chemistry. There are several reactions in this scheme that reduce the efficiency of acetic acid formation through this mechanism, notably the following:

1. The formation of excited Criegee intermediates that do not survive long enough to participate in the reaction with water and its dimer
2. The primary ozonide may form the formaldehyde oxide Criegee intermediate, which will not lead to direct formation of acetic acid
3. The *syn*-acetaldehyde oxide and *anti*-acetaldehyde oxide can undergo isomerization, with the former leading to a vinyl hydroperoxide (a nonacetic acid-producing channel) and the latter producing excited acetic acid, which can decompose before it is collisionally stabilized.

The importance of processes 1 and 2 are defined by the alkene that is undergoing ozonolysis, with yields of excited versus stabilized and acetaldehyde versus formaldehyde oxide varying with the types of substitution about the olefinic bond. The importance of 3 depends upon the rates of the isomerization reactions and how they compete with the reaction with water and its dimers and are therefore dependent not only on the rate coefficients of these processes but also the relative humidity.

In polluted urban environments, the reactions of peroxyacetyl species (RCO_3) with NO_2 are dominant, producing peroxyacyl nitrates—one of the components of photochemical smog. However, in rural environments or areas with only moderate levels of pollution, the reactions of peroxyacetyl radicals with HO_2 and RO_2 can produce a significant amount of CH_3COOH (Jacob & Wofsy, 1988; Madronich & Calvert, 1990):

$$CH_3CO_3 + HO_2 \rightarrow CH_3COOH + O_3 \quad (1)$$

$$CH_3CO_3 + RO_2 \rightarrow CH_3COOH + O_2 + \text{other products} \quad (2a)$$

$$\rightarrow CH_3COO + O_2 + \text{other products} \quad (2b)$$

Reaction (2a) is very slow (~10%) compared with the reaction (2b) at room temperature. However, a significant amount of CH_3CO_3 (reaches up to ~4 ppt in the tropics) and RO_2 (consisting CH_3O_2 and an additional 46 organic peroxy radicals reach up to 40 ppt in the tropics) can exist in the atmosphere (Khan, Cooke, Utembe, Archibald, Derwent, et al., 2015) and therefore reaction (2a) is anticipated to be a significant source of CH_3COOH in clean tropospheric environments.

By virtue of the low reactivity of CH_3COOH, its removal from the troposphere by chemical reactions occurs slowly and its major sinks in the atmosphere are dry and wet deposition (Seco et al., 2007). Precise estimates for dry and wet deposition rates of CH_3COOH are of importance as its tropospheric lifetime is strongly controlled by the deposition loss (Chebbi & Carlier, 1996). However, recent studies (Chhantyal-Pun et al., 2017; Welz et al., 2014) suggested a very rapid chemical reaction of Criegee intermediates with carboxylic acids. Therefore, it is possible that the role of gas phase loss processes has been underestimated by previous studies.

There are a few modeling studies, for example, MOGUNTA by Baboukas et al. (2000), MATCH-MPIC by von Kuhlmann et al. (2003), IMPACT by Ito et al. (2007), and GEOS-Chem by Paulot et al. (2011) where the global budgets of CH_3COOH have been explored. The most detailed global budget of CH_3COOH is presented by Paulot et al. (2011), where they produced bottom-up estimates of the global sources of CH_3COOH following the construction of an updated emissions inventory and chemical scheme and evaluated the model results against an extensive array of ground, ship, satellite, and flight campaign data. The GEOS-Chem model encapsulates the seasonality of CH_3COOH concentrations well but generally underestimates their tropospheric levels indicating an undefined source of atmospheric CH_3COOH (Paulot et al., 2011).

The global budget and distribution of CH_3COOH are not well reproduced in global atmospheric models because of the poor inventory of sources and sinks (Rosado-Reyes & Francisco, 2006; Singh et al., 2000). This is a consequence of the lack of clarity in the relative importance of known sources or the possible importance of unknown sources and/or errors in the sink processes of CH_3COOH at a regional and global scale and several studies highlight sizeable discrepancies between model and measurement data (Ito et al., 2007; Paulot et al., 2011; von Kuhlmann et al., 2003). Therefore, an investigation into the tropospheric chemistry of CH_3COOH using the global 3-D chemistry transport model STOCHEM-CRI has been undertaken. The simulations are performed with updates to the chemical mechanism (e.g., water complexation of peroxy radicals and their subsequent reactions with CH_3CO_3, SOA oxidation, loss of CH_3COOH by Criegee) and emissions inventory of the species (e.g., acetaldehyde and isoprene) of the model, and comparisons of the results made with other modeling studies as well as surface stations and flight campaigns measurement data. The relevance of the reaction of gas phase CH_3COOH with Criegee intermediates as a potential loss process of CH_3COOH has also been explored and is unaccounted for in the previous modeling studies.

2. Model Description

The 3-D global chemical transport model employed during this investigation was that of STOCHEM. An original version of the model was presented by Collins et al. (1997) with updates detailed in Derwent et al. (2008). STOCHEM is an "offline" model driven by archived meteorological data. The meteorological data were generated by the UK Met Office Unified Model at a climate resolution of 1.25° longitude × 0.83° latitude × 12 vertical levels up to a boundary of 100 hPa (Johns et al., 1997). Parameters incorporated in the data include temperature, wind, humidity, pressure, tropopause height, clouds, surface parameters, and boundary layer depth.

STOCHEM advects 50,000 constant mass air parcels using a Lagrangian approach such that the chemistry and transport processes are uncoupled. Within each of the parcels, chemical species are produced and lost in chemical reactions and photochemical dissociations. Physical processes acting on chemical species within the parcels include emissions, dry and wet deposition, convection, and subgrid scale mixing between air parcels (Derwent et al., 2003). The chemical mechanism used in STOCHEM is the common representative intermediates mechanism version 2 and reduction 5 (CRI v2-R5). The detail of the CRI v2-R5 mechanism is given by Jenkin et al. (2008), Watson et al. (2008), and Utembe et al. (2009). Further amendments to the chemical mechanism and a description of the addition of an organic aerosol module are reported by Khan, Jenkin, et al. (2017). The chemical scheme comprises 244 chemical species that take part in 564 chemical reactions

and 98 photolysis reactions. The concentration of each chemical species is updated using a backward Euler integration with an advection chemical time step of $\Delta t = 5$ min (Collins et al., 1997). The photolysis rate for any given reaction is determined explicitly for each individual parcel with a time resolution of 1 hr. These rates are subsequently interpolated linearly to achieve the 5-min resolution values required for the chemical integration. More details about the photolysis scheme implemented in the model can be found in Khan, Cooke, Utembe, Archibald, Maxwell, et al. (2015).

Emissions within STOCHEM are characterized into three different types: surface, stratospheric, and three-dimensional emissions. Surface emissions from ocean, soil, vegetation, and biomass burning are distributed using two-dimensional source maps at a resolution of 5° longitude × 5° latitude (Olivier et al., 1996), which varies by calendar month. Emissions totals for nitrogen oxides, carbon monoxide, and nonmethane volatile organic compounds for the year 1998 are taken from the Precursors of Ozone and their Effects in the Troposphere inventory (Granier et al., 2005). Further details of the STOCHEM emissions inventory for all species can be found in Khan et al. (2014).

Dry deposition is accounted for using a resistance approach in STOCHEM and the rate at which it occurs depends on whether it is over land or ocean with relevant species-dependent deposition velocities for both. The dry deposition velocities of CH_3COOH over land and ocean were considered as 1.30 and 1.34 cm/s, respectively (Helas et al., 1992), which were used in all simulations. Wet deposition is represented in STOCHEM through the use of species-dependent scavenging coefficients. The dynamic scavenging of 2.0 cm^{-1} and convective scavenging of 4.0 cm^{-1} for CH_3COOH are determined from a relationship plot of Henry's law solubility coefficients (taken from Sander, 2015) and scavenging coefficients (taken from Penner et al., 1994) for a suite of species. These scavenging coefficients are combined with scavenging profiles and precipitation rates to calculate the wet deposition loss rates for CH_3COOH from an air parcel.

Four simulations were performed during the study: STOCH-Base, STOCH-AO, STOCH-WC, and STOCH-IM. The simulation, STOCH-Base, was based on the reference conditions described in Khan, Jenkin, et al. (2017) with additional amendments of the global emissions of CH_3COOH (anthropogenic: 9.67 Tg/year, biomass burning: 11.23 Tg/year, soil: 3.48 Tg/year, and vegetation: 2.58 Tg/year) taken from Paulot et al. (2011). The rate coefficients and branching ratios for the production and loss reactions were extracted from the Master Chemical Mechanism website (http://mcm.leeds.ac.uk/MCM/). More details about the production and loss processes implemented in the model can be found in supporting information (Table S1; Butkovskaya et al., 2006; McGillen et al., 2017; Vereecken et al., 2017). Acetaldehyde is one of the major precursors of CH_3COOH, which has a strong oceanic source; therefore, a simulation, STOCH-AO, was conducted by including the global emissions of acetaldehyde (oceanic: 57 Tg/year, biomass burning: 3 Tg/year, anthropogenic: 2 Tg/year, and biogenic: 23 Tg/year) into STOCH-Base based on the emissions inventory reported by Millet et al. (2010). An oceanic emission of isoprene (top-down estimate of 1.9 Tg/year by Arnold et al., 2009) was also included in the STOCH-AO simulation. The complexation of HO_2 and RO_2 radicals with water vapor molecules (Clark et al., 2008; Kanno et al., 2006) accelerate the reaction with CH_3CO_3 producing higher CH_3COOH. Thus, in the third simulation STOCH-WC, the reactions of water complexed HO_2 and RO_2 with CH_3CO_3 were considered with a factor of 2 increment of the rate coefficients of the reactions (Khan, Cooke, Utembe, Archibald, Derwent, et al., 2015). Isoprene is another major precursor of CH_3CO_3; a further simulation, STOCH-IM, was conducted with updating global vegetation emissions of isoprene (594 Tg/year) reported by Sindelarova et al. (2014). All simulations were conducted with meteorology from 1998 for a period of 24 months with the first 12 allowing the model to spin up. Analysis is performed on the subsequent 12 months of data. The Criegee chemistry was integrated in STOCH-IM to calculate the steady state concentration of stabilized Criegee Intermediates (sCIs) by including the production of the Criegee intermediate (CI) from the ozonolysis reactions of six alkenes (e.g., ethene, propene, t-but-2-ene, isoprene, α-pinene, and β-pinene) using the rate coefficients taken from the Master Chemical Mechanism (http://mcm.leeds.ac.uk/) and their individual loss through unimolecular, water, water dimer, and CH_3COOH reactions. The rate coefficients of the loss of Criegee by unimolecular, water, and water dimer can be found in McGillen et al. (2017). The rate coefficient of the loss of Criegee by CH_3COOH can be found in the supporting information (Table S2; Chhantyal-Pun et al., 2018; Khan et al., 2018; Welz et al., 2014). The CH_3COOH lost by reaction with Criegee intermediates is determined as a percentage of the total theoretical amount of CH_3COOH lost via the all chemical reactions and physical process (e.g., deposition).

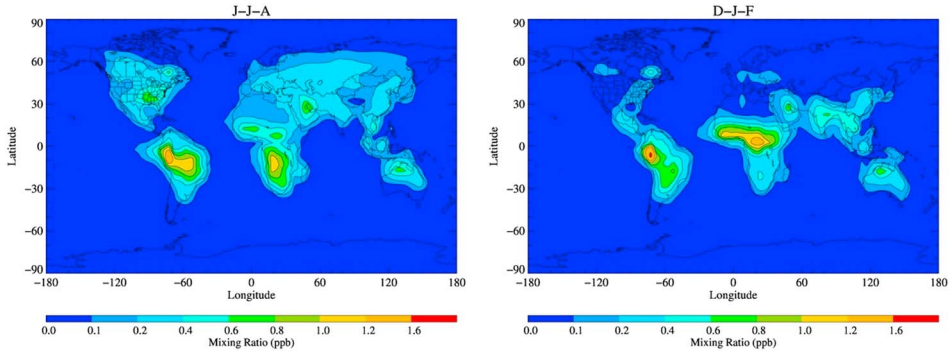

Figure 1. The surface level distribution of CH_3COOH simulated by the STOCH-Base for June-July-August (J-J-A) and December-January-February (D-J-F) seasons.

3. Results and Discussion

3.1. Surface Distribution

Figure 1 shows the surface distributions of CH_3COOH concentrations in the STOCH-Base simulation during June-July-August (J-J-A) and December-January-February (D-J-F) seasons. The plots show higher CH_3COOH concentration in the tropical regions, with the highest in South America and Southern Africa in J-J-A and South America and central Africa in D-J-F.

The CH_3COOH hot spots in the tropics are found with mixing ratios by as much as 1.6 ppb in South America (Figure 1). These hot spots can be ascribed to the large quantities of CH_3COOH produced by the reactions (1) and (2a) in these regions. Peroxyacetyl radicals are abundant in the atmosphere over South America due to the large quantities of biogenic volatile organic compound precursors that are released from the forest. Isoprene is one of the predominant precursors to CH_3CO_3 and has a large emission flux in these regions. In addition, the relatively unpolluted section of the troposphere above the forest contains moderately low levels of nitrogen oxides pollutants of about 500 pptv. Therefore, the abundant CH_3CO_3 are not consumed by reactions with nitrogen oxides but instead react with HO_2 and RO_2 radicals to generate CH_3COOH.

The higher concentrations of CH_3COOH are found during the dry season due to a slower loss rate owing to lower levels of deposition and corresponding lower concentrations during the wet season. This is indeed the case in Figure 1 for the northern parts of South America (e.g., Brazil) with comparatively higher CH_3COOH concentrations during the dry season (J-J-A) and the comparatively lower CH_3COOH concentrations during the wet season (D-J-F). Similar agreement between dry and wet seasons and CH_3COOH concentrations exists for the other hot spots of CH_3COOH located in Africa. For countries in central Africa (e.g., Central African Republic) the dry season falls between December and February and the wet season lies between July and September but Angola, located on the west coast of Southern Africa, has distinct dry (J-J-A) and wet (D-J-F) seasons. Thus, the higher CH_3COOH concentrations are found in central Africa and Southern Africa during D-J-F and J-J-A, respectively.

Including the oceanic emissions of acetaldehyde and isoprene in STOCH-AO increases by 8.9 Tg/year CH_3COOH chemical production globally which increases the concentration of CH_3COOH relative to the STOCH-Base by up to 30 ppt (400%) at the equator in the Pacific and Indian Ocean during J-J-A season and up to 25 ppt (700%) over the Southern Hemisphere (SH) oceans during D-J-F season (Figure 2). The large secondary production of CH_3COOH from acetaldehyde and isoprene in the marine environment confirms the significant source of CH_3COOH over the oceans.

The zonal distribution plot shows that the peaks of CH_3COOH (up to 0.20 ppb) are found at the tropics because of larger biogenic emissions within this region (Figure 3a). The high levels of CH_3COOH (up to 0.1 ppb) at the top of the model domain in STOCH-Base are found in the tropics because of the ubiquitously distributed CH_3CO_3 throughout the troposphere after forming from the oxidation of most nonmethane volatile organic compounds (VOCs). The secondary production of CH_3COOH from oceanic sources in STOCH-AO increases the CH_3COOH concentration by up to 250% in the SH oceans (Figure 3b). The oceanic acetaldehyde

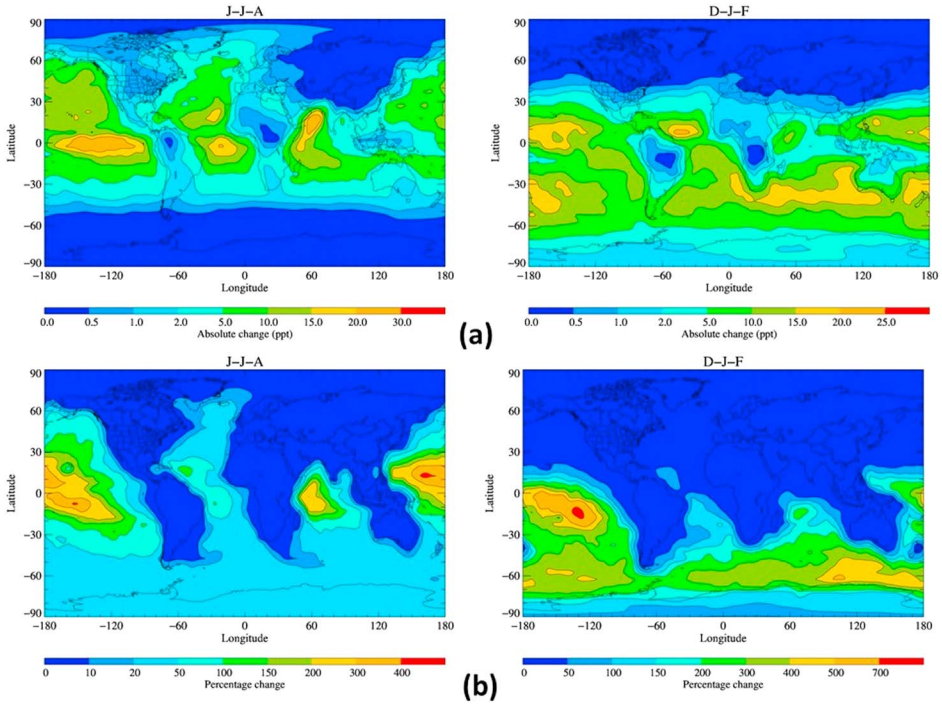

Figure 2. (a) Absolute changes and (b) percentage changes of surface CH_3COOH concentration from STOCH-Base to STOCH-AO simulation during December-January-February (D-J-F) and June-July-August (J-J-A) seasons.

and isoprene emissions can produce large amounts of CH_3CO_3 and peroxy radicals resulting in increasing the mixing ratios of CH_3COOH in these regions.

An increase of 12% in the CH_3COOH level was found in the marine environment after considering the water complexation of peroxy radicals and the subsequent reactions of the water complexed HO_2 and RO_2 with CH_3CO_3 (Figure 4a). Upon updating the emission inventory of isoprene in the STOCH-IM simulation gave a further increase (up to 20%) of surface CH_3COOH over the forested regions of South America, South Africa and Australia (Figure 4b) because of the increased formation of CH_3CO_3 from the oxidation of isoprene.

3.2. Model-Measurement Comparison

The comparison between measurement and model is not straight forward for CH_3COOH and several caveats must be kept in consideration. The meteorological data for the year 1998 was used in the model; thus, the meteorology can have impact on the model values when compared with measured data for other years. Year 1998 was an El Niño year, but the emissions of CH_3COOH (especially biomass burning event) were

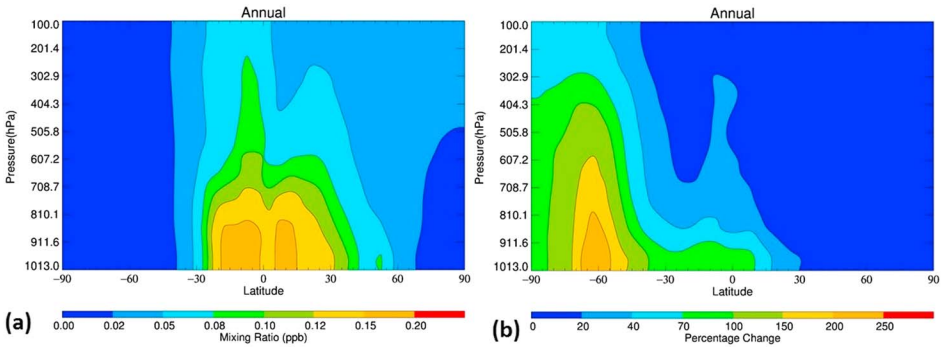

Figure 3. The zonal distribution of (a) the annual CH_3COOH concentration for the STOCH-Base simulation; (b) the percentage change of annual CH_3COOH concentration from STOCH-Base to STOCH-AO simulation.

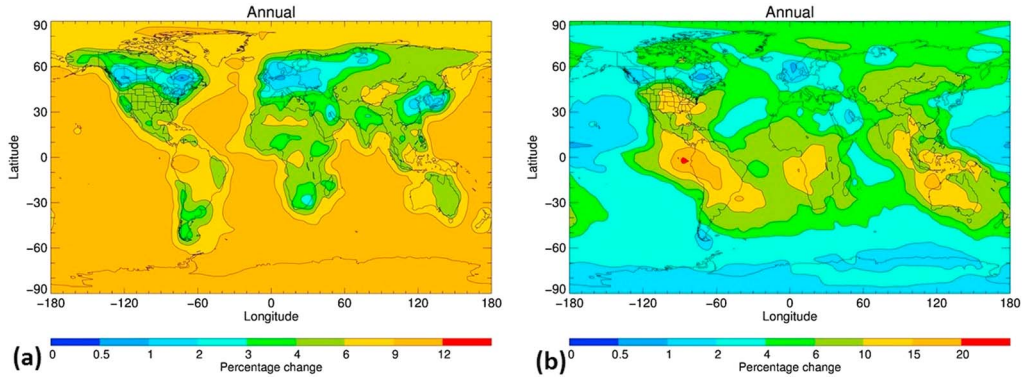

Figure 4. The annual percentage change of surface CH_3COOH concentration from (a) STOCH-AO to STOCH-WC and (b) STOCH-WC to STOCH-IM.

not tied to 1998 which could lead to additional biases when compared with transition and La Niña years. The measured data used in the comparison are mostly from the offline method technique such as aqueous scrubber or mist chamber techniques for collecting the sample and ion exchange chromatography or Liquid Chromatography for analyzing CH_3COOH; the sampling techniques can be subject to measurement bias as a result of signal artifacts due to production and loss from various sampling media. The development of a network of gas phase measurements of acetic acid would be extremely useful in assisting the constraint of acetic acid levels in global models. A limited number of olefins producing CH_3COOH through Criegee intermediate, CH_3CHOO formation, are used in the model because of the lack of their emission inventories. Khan, Morris, et al. (2017) found the most abundant Criegee to be CH_3CHOO (73%) among all other Criegee Intermediates in the UK urban environment. The dominating precursors of CH_3CHOO were found in their study to be 2-methyl-2-butene (49%), trans-2-butene (17%), cis-2-butene (11%), trans-2-pentene (5%), propene (5%), cis-2-pentene (2%), 4-methyl-trans-2-pentene (2%), 3-methyl-trans-2-pentene (2%), 3-methyl-cis-2-pentene (3%), and trans-2-hexene (1%). Our model only includes trans-2-butene and propene which is only 22% for the total contribution of the formation of CH_3CHOO; this can make the model performance unsatisfactory. The surface sites measure a range of polluted and unpolluted air masses, depending on the meteorology, which makes it difficult to compare the modeled data with the measurement data. The coarse model resolution (5° × 5°) is responsible for poorer model performance over polluted regions because they cannot represent typical biomass burning plumes or regional pollution correctly. More details about the uncertainty of the model can be found in Khan et al. (2014), Khan, Cooke, Utembe, Archibald, Derwent, et al. (2015), Khan, Cooke, Utembe, Archibald, Maxwell, et al. (2015), Khan, Cooke, et al. (2017), and Khan, Jenkin, et al. (2017).

In the study, a comparison of modeled vertical profiles of CH_3COOH with aircraft measurements was conducted for four designated campaigns (Figure 5). The SONEX, PEM Tropics-B, ITCT2K4, and TexAQS II studies compiled from Ito et al. (2007), von Kuhlmann et al. (2003), and Paulot et al. (2011) were selected for model-measurement comparison. More details of the measurement sites can be found in supporting information (Table S3). There was a general underprediction of CH_3COOH by the model over all altitudes (mean bias of 0.05 ppb for STOCH-Base simulation). An improvement in the accuracy of the model with the reduction of mean biases of 14%, 6%, and 16% is apparent for all flight data following the updating the acetaldehyde emission inventory in STOCH-AO, increasing rate of the reaction of $CH_3CO_3 + HO_2/RO_2$ due to water complexation of peroxy radicals in STOCH-WC and updating the isoprene emission inventory in STOCH-IM, respectively.

The vertical profile of CH_3COOH for remote oceans in STOCH-AO (Figure 5) shows a significant increase of the model CH_3COOH in the Tropical Pacific, Easter Island, Hawaii, Christmas Island and a slight increase in the Tahiti and Fiji. A further improvement of the model CH_3COOH in the tropical oceans are seen in STOCH-WC due to the complexation of peroxy radicals with water resulting in faster rates of peoxy-peroxy radical reactions. The concentrations of $RO_2.H_2O$ in tropical areas are as high as 5 ppt, which correspond to approximately 12% of the peroxy radicals (Khan, Cooke, Utembe, Archibald, Derwent, et al., 2015). The formation of complexes of peroxy radicals with water reduce the energy barrier of the transition state for the

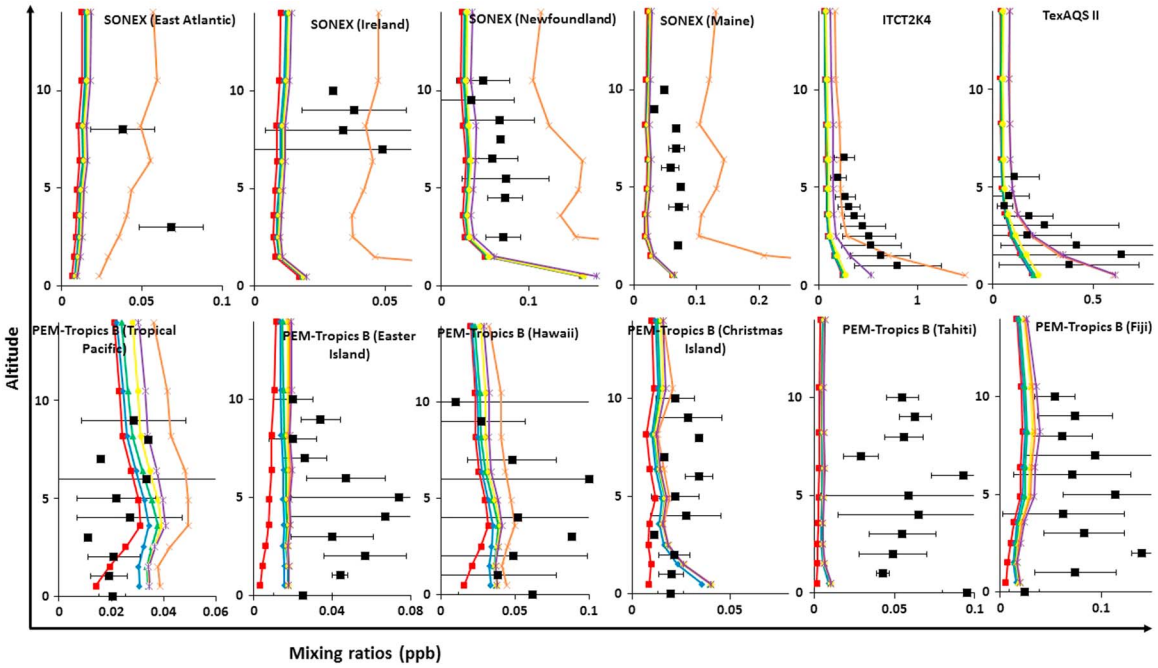

Figure 5. Vertical profiles for measured CH_3COOH using aircraft data from the SONEX, PEM Tropics-B, ITCT2K4, and TexAQS II flight campaigns and modeled CH_3COOH using STOCHEM model. Red squares, blue diamonds, green triangles, yellow rounds, violet stars, and orange crosses represent the model data for STOCH-Base, STOCH-AO, STOCH-WC, STOCH-IM, STOCH-BIO, and STOCH-ANTH simulations, respectively. Black squares represent measurement data and the black error bars represent measurement variability.

peroxy-peroxy radical reaction, which enhance the formation of CH_3COOH in the tropical oceans. Despite an increase in CH_3COOH concentration between the STOCH-Base and STOCH-AO simulations, the STOCH-AO concentrations remain up to twofold to threefold lower than the measured concentrations for Fiji and Tahiti. One of the possible reasons for the large discrepancies may be the sample air mass which was affected by a biomass burning plume from Southeast Asia or Australia during the PEM Tropics-B campaign.

The location of Ireland is such that the atmospheric composition is heavily impacted by SW prevailing winds and is therefore representative of marine Atlantic air. Adding the oceanic emissions in STOCH-AO still underpredicts the concentration of CH_3COOH in Atlantic oceans. These comparisons emphasize the need for further investigation into the origins of CH_3COOH in the troposphere, with a focus on midlatitudinal oceanic regions. Further data were collected over Maine in the United States and Newfoundland in Canada as part of the SONEX study. A similar increase in CH_3COOH concentration persists over the four STOCHEM simulations, and the model underpredicts when contrasted with measurement data. One possible explanation is higher anthropogenic emissions of CH_3COOH in the northeastern United States and Canada than are predicted in the emissions inventory. The underprediction is also visible for the campaigns, TexAQS and ITCT2K4, which were heavily influenced by anthropogenic pollution and anthropogenic + biomass burning plumes, respectively. Acetic acid can be produced from vinyl alcohol (Archibald et al., 2007), which are likely to be produced from combustion sources (anthropogenic or biomass). Inclusion of vinyl alcohols and their chemistry in STOCHEM-CRI can reduce the discrepancy between model and measured CH_3COOH in these campaign sites.

In general, the model runs, STOCH-Base, STOCH-AO, STOCH-WC, and STOCH-IM, produce a better model-measurement comparison for tropical region compared with midlatitudinal regions. We compared midlatitudinal (e.g., East Atlantic, Ireland, Newfoundland, Maine, ITCT2K4, and TexAQS II) measured CH_3COOH with model CO (tracer for anthropogenic and biomass burning emissions) and found an excellent correlation (R^2 = 0.83) between them (Figure S1). A sensitivity experiment was conducted with an arbitrary additional anthropogenic emission of CH_3COOH (100 Tg/year) introduced to STOCH-IM in a run hereafter referred to as *STOCH-ANTH* (orange lines in Figures 5 and 6). The vertical profiles of SONEX, TexAQS, and ITCT2K4 flight campaigns show a significant increase of tropospheric CH_3COOH in STOCH-ANTH, which brings the model into closer agreement with most of the measurements suggesting that there could be significant amount

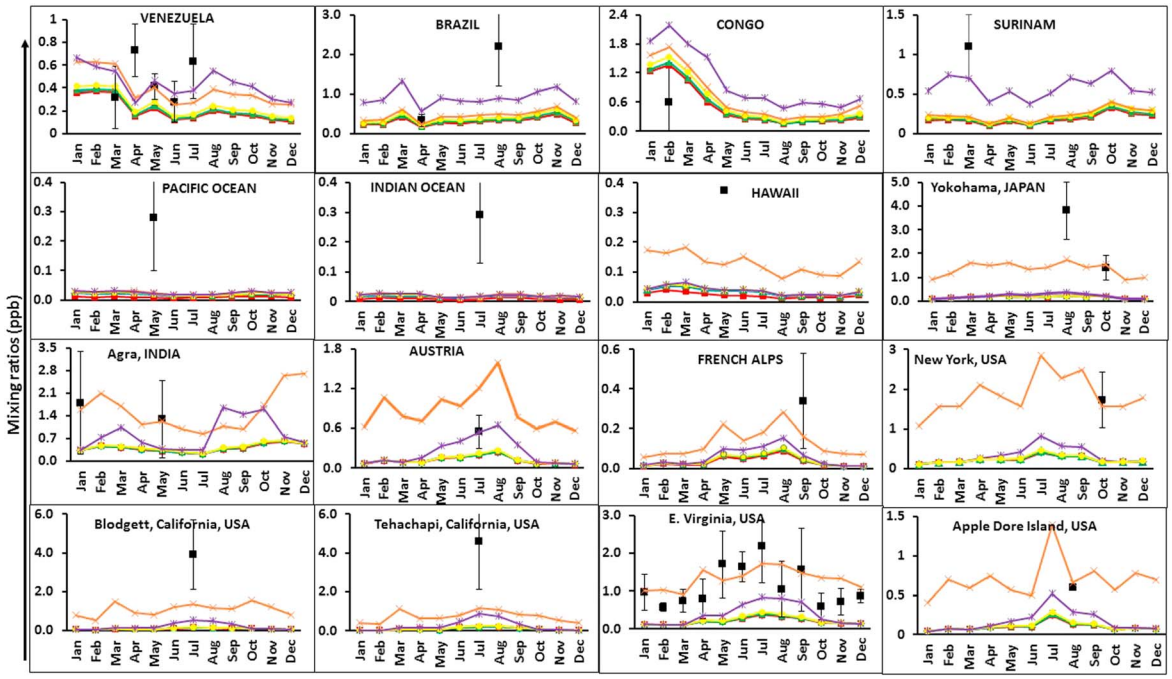

Figure 6. The monthly variation of model and measured CH_3COOH mixing ratios. Red squares, blue diamonds, green triangles, yellow rounds, violet stars, and orange crosses represent the model data for STOCH-Base, STOCH-AO, STOCH-WC, STOCH-IM, STOCH-BIO, and STOCH-ANTH simulations, respectively. Black squares represent measurement data, and the black error bars represent measurement variability.

of anthropogenic direct emissions of CH_3COOH or anthropogenic precursors with large yields of CH_3COOH which were not considered in our model.

Figure 6 presents the model results for all simulations alongside measurement data from 16 surface station sites situated in different environments across the globe. More details about the measurement sites can be found in supporting information (Table S4; Andreae et al., 1988; Arlander et al., 1990; Haase et al., 2012; Harrington et al., 1993; Helas et al., 1992; Khwaja, 1995; Kumar et al., 1996; Norton, 1992; Preunkert et al., 2007; Puxbaum et al., 1988; Quesada et al., 2001; Sanhueza et al., 1996; Schultz Tokos et al., 1992; Talbot et al., 1988). Talbot et al. (1988) monitored the gas phase atmospheric concentration of CH_3COOH over a 15-month period at a site in eastern Virginia. Data from this study for each of the 12 months of the year are plotted alongside concentrations from the STOCHEM simulations in Figure 6. This plot provides a useful insight into how well STOCHEM replicates the seasonality of CH_3COOH at a given location. In the field campaign, a marked annual seasonality was noted with higher concentrations in the growing season (March–September) than the nongrowing season (October–February). Peak concentrations were registered in the summer month of July. The model data display moderate agreement with the trend in measurement data, replicating lower levels of CH_3COOH in the winter months of December, January, and February, and generate much higher concentrations in the peak growing season months of June-July-August. However, there is a large disagreement between model-measurement data throughout the year with a twofold to threefold lower CH_3COOH level in model data than that in measurement data. A good correlation is found (R^2 = 0.61) between measured CH_3COOH and model isoprene (tracer of biogenic emissions) for this site (Figure S2). A sensitivity experiment was conducted to investigate the missing biogenic sources of acetic acid by considering an arbitrary addition of biogenic emissions of 50 Tg/year to STOCH-IM in a run refereed as STOCHEM-BIO (violet lines in Figures 5 and 6). The model-measurement agreement has been improved significantly for the forested and rural sites (e.g., Los Caracas, Venezuela; Amazonia region, Brazil; Surinam; Eastern Virginia, United States) when additional biogenic emission is included; this supports the importance of unknown biogenic precursors with large yields of CH_3COOH which were not considered in the model.

Sanhueza et al. (1996) measured the gas phase concentration of CH_3COOH at a number of sites in Venezuela during the dry and wet seasons. Average monthly concentrations from a coastal site at Los Caracas are

compared here with the STOCHEM simulation data. Good agreement is found between model and measurement data with simulated concentrations falling within the measurement data error bars (see Figure 6). The model-measurement agreement is also found to be reasonable for the DECAFE experiment and ICARTT campaign where the CH_3COOH was measured from the tropical forest of the People's Republic of the Congo in February 1988 (Helas et al., 1992) and from the Appledore Island, ME, United States, in July–August 2004 (Haase et al., 2012). Excellent agreement is observed between model and measurement data recorded during April–May of the 1987 wet season at a site in the Amazonian region in Brazil (Talbot et al., 1990). In addition to the high concentrations of peroxyacetyl radicals and peroxy radicals in the Amazonian region, there are persistently high relative humidity levels. Thus, STOCH-WC brings the model into closer agreement with measurement at this site during the wet season. However, the model underpredicts CH_3COOH abundances relative to measurement data recorded during the dry season at this site. The increased isoprene emissions in STOCH-IM slightly increase the CH_3COOH concentration, but model data remain up to twofold to threefold lower than the measured data during dry season. It is possible that the biomass burning in the dry season exceeds the emissions predicted in our model and is responsible for the higher measurement data concentrations.

Data for the Pacific Ocean and Indian Ocean sites have been taken from a cruise of the SH Pacific Ocean and Indian Ocean by Arlander et al. (1990) during which the measurements of CH_3COOH were recorded. The measurement points at 0.28 ppb and 0.29 ppb represent the average concentration of CH_3COOH in SH Pacific Ocean and Indian Ocean recorded for this leg of the cruise. A slight increase in CH_3COOH concentration is simulated at the SH Pacific and Indian Oceans when the oceanic emissions of acetaldehyde and isoprene are considered in STOCH-AO. However, the model still underpredicts CH_3COOH concentrations relative to the measurement data. There are several possible explanations for this. First, there may be direct oceanic sources of CH_3COOH, which have not been accounted for in the STOCHEM model and are contributing to the higher concentrations of CH_3COOH observed in the measurement data. Second, there may be other secondary sources of CH_3COOH (e.g., the degradation of marine organic aerosol; Keene et al., 2015) that are not included in STOCHEM. In the study, the average CH_3COOH mixing ratio values for the cruise were used for the model validation, so there is a possibility several of the values at higher latitudes were impacted by anthropogenic emissions, or biomass burning plumes. Paulot et al. (2011) also observed their model underpredicted CH_3COOH concentrations in remote marine environments and therefore further investigations of these discrepancies are highly desirable.

The model-measurement agreement is also found to be within one standard deviation of the mean measured values for the semirural site in Agra, India, during the winter and summer (Kumar et al., 1996) and for the Vallot observatory in French Alps (4,360 m above sea level) during September 2004 (Preunkert et al., 2007). Puxbaum et al. (1988) measured the gas phase concentration of CH_3COOH at three sites in eastern and northern Austria. Unlike the previous stations discussed, the values of the concentrations for all model runs are similar in magnitude for the station in Austria, with concentrations from the simulations found to be highest for August. The concentrations of NO_2 over mainland Europe are expected to be higher than those of the previous remote/rural sites discussed and therefore most of the peroxyacetyl radicals present in the troposphere react preferentially with NO_2 species to form peroxyacyl nitrate. Thus, they are not participating in reactions that produce CH_3COOH in these regions.

A similar trend in these data exists for the modeled concentrations of CH_3COOH over Japan, New York, United States, and California, United States. Output concentrations from all simulations are found to be similar in magnitude. While the model underpredicts abundances for the site in Austria by a factor of 2, the modeled concentrations for Japan, New York, and California are significantly lower than the measurement data points. The measurement data points for Japan and New York represent the average concentrations of CH_3COOH measured on a particular day in August and October at an urban site in Yokohama, Japan, and a semiurban site in New York, United States. The measured data points for California are representative of the concentrations of CH_3COOH for forested regions of the Sierra Nevada that are impacted by pollutants generated in the central valley region of California (Harrington et al., 1993). It is probable that the local anthropogenic emissions from motor exhaust emissions and industrial sites can be responsible for the high CH_3COOH concentrations recorded during these three studies. We found a good correlation between measured CH_3COOH and model n-butane (tracer of anthropogenic emissions) for the urban sites (e.g., Yokohama, Japan, New York, United States, California, United States, and Austria; Figure S3). The additional anthropogenic emissions of

Table 1
Global Budget of CH_3COOH

CH_3COOH	STOCH-Base	STOCH-AO	STOCH-WC	STOCH-IM	STOCH-ANTH	STOCH-BIO	Paulot et al. (2011)	von Kuhlmann et al. (2003)	Ito et al. (2007)	Baboukas et al. (2000)
Sources										
Direct Emission	26.9 (26)	26.9 (24)	26.9 (23)	26.9 (20)	126.9 (54)	76.9 (42)	26.9 (31)	18.0 (19)	31.0 (42)	47.9 (29)
Chemical Production	75.9 (74)	84.8 (76)	91.8 (77)	107.4 (80)	107.2 (46)	107.1 (58)	58.6 (69)	75.0 (81)	42.0 (58)	120.0 (71)
Total sources	102.8	111.7	118.7	134.3	234.1	184.0	85.5	93.0	73.0	167.9
Sinks										
OH Removal	22.4 (22)	23.5 (21)	25.1 (21)	27.7 (21)	42.1 (18)	34.9 (19)	24.8 (29)	N/A	N/A	N/A
Dry Deposition	25.8 (25)	28.5 (26)	29.8 (25)	32.5 (24)	84.2 (36)	55.2 (30)	31.4 (36)	N/A	N/A	N/A
Wet deposition	54.6 (53)	59.7 (53)	63.8 (54)	74.1 (55)	107.6 (46)	92.0 (51)	27.1 (32)	N/A	N/A	N/A
Dust	N/A	N/A	N/A	N/A	N/A	N/A	2.4 (3)	N/A	N/A	N/A
Global burden (Tg)	0.45	0.51	0.54	0.61	1.11	0.88	0.55	N/A	N/A	N/A
Lifetime (days)	1.6	1.7	1.7	1.7	1.8	1.8	2.3	N/A	N/A	N/A

Note. The flux values are in Tg/year. The percentage contributions are shown in parentheses, and N/A represents no available data.

CH_3COOH in STOCH-ANTH reduce the discrepancies significantly between model and measurements for these sites (Figure 6) supporting that there could be large unknown anthropogenic emissions of CH_3COOH either directly or through secondary production from the anthropogenic precursors.

The photochemical degradation of secondary organic aerosol can be another source of CH_3COOH in the urban areas (Malecha & Nizkorodov, 2016; Pan et al., 2009; Sareen et al., 2013). Considering the photolysis rate of SOA as $J_{SOA} = 4 \times 10^{-4} J_{NO2}$ (Hodzic et al., 2015) yielding 100% CH_3COOH, we examined the production of CH_3COOH from the photodegradation of SOA from the STOCHEM model run (referred to as STOCH-ASOL) and found a negligible amounts of CH_3COOH production globally (100 kg/year) from this reaction channel. The heterogeneous oxidation process can be a substantial sink of SOA mass in the troposphere (Hodzic et al., 2016). If we consider the lifetime of organic particles toward heterogeneous oxidation is 2 days (Molina et al., 2004) and the oxidation process produces 100% CH_3COOH, the STOCHEM simulation (STOCH-ASOL) produces a further 205 kg/year of CH_3COOH.

3.3. Global Budget

Table 1 presents the global budget of CH_3COOH for the six simulations performed during this investigation, in addition to the global budget from Paulot et al. (2011), von Kuhlmann et al. (2003), Ito et al. (2007), and Baboukas et al. (2000). In all simulations presented in the study, the direct emissions only represent 20–26% of the total sources, which are in excellent agreement with the study of Paulot et al. (2011), von Kuhlmann et al. (2003), and Baboukas et al. (2000; see Table 1). The large percentage production contribution (74–80%) from chemical reactions dominated by $CH_3CO_3 + HO_2$ and $CH_3CO_3 + RO_2$ in the simulations (STOCH-Base, STOCH-AO, STOCH-WC, and STOCH-IM) highlights the importance of the peroxyacetyl radical in the production of CH_3COOH in the troposphere.

Total CH_3COOH sources of 102.8 Tg/year in the STOCH-Base simulation were found to be higher than the studies of Paulot et al. (2011), von Kuhlmann et al. (2003), and Ito et al. (2007) who estimated sources to be 85.5, 93.0, and 73.0 Tg/year, respectively. The better representation of CH_3CO_3 during oxidation of biogenic VOC (e.g., isoprene) in the STOCH-Base (Khan, Cooke, et al., 2017) gives a chemical production of CH_3COOH (75.9 Tg/year). The updated acetaldehyde emission inventory in STOCH-AO, the rate enhancement of the reaction of $CH_3CO_3 + HO_2/RO_2$ due to water complexation of HO_2 and RO_2 in STOCH-WC, and the updated isoprene emission inventory in STOCH-IM increase the chemical production of CH_3COOH to 84.8, 91.8 and 107.4 Tg/year, respectively (Table 1). Baboukas et al. (2000) predicted a total chemical production of atmospheric CH_3COOH of 120 Tg/year, which is much higher than that shown in our study. As von Kuhlmann et al. (2003) explained, it is likely that Baboukas et al. (2000) overpredicted the production of CH_3COOH from the reaction of peroxyacetyl radicals with HO_2 due to the selection of a branching ratio yielding a proportion of CH_3COOH that is too high.

The global sinks of CH_3COOH are dominated by wet deposition (53%) followed by dry deposition (25%) and the loss by OH (22%) for the STOCH-Base simulation. The increased wet deposition loss is associated with the

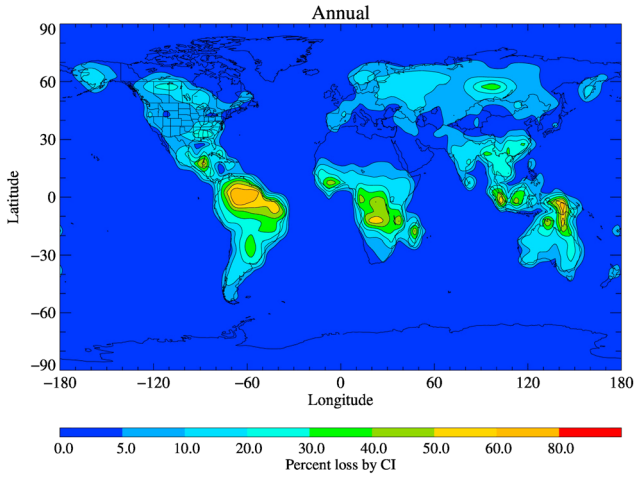

Figure 7. The percent loss of CH_3COOH by Criegee intermediate. Note: Percent loss by CI = (loss of CH_3COOH by CI × 100)/Total loss CH_3COOH. CI = Criegee intermediate.

increased concentrations of CH_3COOH in the tropical rainforest region brought about by their substantial production from peroxyacetyl radical reactions in low NO_x environments. The scavenging coefficients used in the model was estimated from the relationship between Henry's law solubility coefficients and scavenging coefficients of a suit of VOCs. These estimated scavenging coefficients could be overestimated values, which increase the wet deposition loss in our model study compared with Paulot et al. (2011) study. The global burden (0.45–0.61 Tg) of CH_3COOH for all simulations in the study is in best agreement with that of the value from Paulot et al. (2011), but the tropospheric lifetime of CH_3COOH (1.6–1.8 days) is found to be lower than those obtained in the study of Paulot et al. (2011). The model-measurement discrepancies suggest the possible unknown or underestimated sources which can contribute to the global burden of CH_3COOH.

3.4. Loss of CH_3COOH by Criegee Intermediates

Recent studies suggested that the reaction of Criegee intermediates with organic acids may be of importance for the tropospheric chemistry of CH_3COOH (Chhantyal-Pun et al., 2017; Welz et al., 2014). An effort has been made to establish the scale of the potential contribution of these reactions to the tropospheric levels of CH_3COOH. The results illustrate that the reaction of CH_3COOH with Criegee intermediates exceeds 60% of the total chemical loss of CH_3COOH in South America, South Africa, Australia, and parts of Southeast Asia (Figure 7). The high concentrations of CH_3COOH in the Amazon rain forest area coincide with high concentrations of sCI, and their reactions could significantly reduce the atmospheric concentration of CH_3COOH. Chhantyal-Pun et al. (2017) found that these reactions show a relatively small temperature dependence over the temperature range found in the lower troposphere. Incorporating these reactions of Criegee intermediates with CH_3COOH in the model results in reduction of CH_3COOH in the Amazon rain forest area. The identification of this significant loss process of CH_3COOH would indicate that the sources of CH_3COOH are currently underpredicted even further.

4. Conclusion

The production of CH_3COOH from the reactions of the peroxyacetyl radical has been shown to be the principal source of tropospheric CH_3COOH, which is consistent with the results of other studies. CH_3COOH concentration hot spots are located primarily in the tropics owing to the high concentration of peroxyacetyl radicals and low nitrogen oxide concentrations in this region. There is reasonable agreement between the STOCHEM model and measurement data, but the model significantly underpredicts concentrations in urban and biomass burning environments suggesting the potential unknown sources and/or errors in the sink processes of CH_3COOH. The reaction of CH_3COOH with sCIs is shown to be a potentially significant loss process of CH_3COOH in the troposphere. The Criegee intermediates may be responsible for over 60% of the chemical loss of CH_3COOH in South America, South Africa, Australia, and parts of Southeast Asia. Thus, the Criegee intermediates make a significant contribution to the reduction of tropospheric lifetime of CH_3COOH. The highly oxygenated species are likely to be produced from this reaction which can lead to nucleation and secondary organic aerosol (SOA) formation. However, the products of this reaction need further investigation to understand its impact on SOA formation regionally and globally.

Acknowledgments
We thank NERC (grants codes NE/K004905/1 and NE/P013104/1) and Bristol ChemLabS under whose auspices various aspects of this work was funded. M. R. M. is supported by Marie Skłodowska-Curie Individual Fellowships HOMER (702794). The participation of CAT and RLC (and the development and operation of the MPIMS kinetics machine) are supported by the Office of Chemical Sciences, Geosciences, and Biosciences, Office of Basic Energy Sciences, United States Department of Energy. Sandia National Laboratories is a multimission laboratory managed and operated by National Technology and Engineering Solutions of Sandia, LLC., a wholly owned subsidiary of Honeywell International, Inc., for the U.S. Department of Energy's National Nuclear Security Administration under contract DE-NA0003525 (The Advanced Light Source is supported by the Director, Office of Science, Office of Basic Energy Sciences, of the U.S. Department of Energy under contract DE-AC02-05CH11231). The views expressed in the article do not necessarily represent the views of the U.S. Department of Energy or the United States Government. All flight and field measurement data sets used in this paper are properly cited and referred to in the reference list. Supporting data for model runs are included as four tables in the supporting information file; any additional data can be obtained from the authors upon request (anwar.khan@bristol.ac.uk).

References

Andreae, M. O., Talbot, R. W., Andreae, T. W., & Harriss, R. C. (1988). Formic and acetic acid over the Central Amazon Region, Brazil 1. Dry season. *Journal of Geophysical Research*, *93*, 1616–1624.

Archibald, A. T., McGillen, M. R., Taatjes, C. A., Percival, C. J., & Shallcross, D. E. (2007). Atmospheric transformation of enols: A potential secondary source of carboxylic acids in the urban troposphere. *Geophysical Research Letters*, *34*, L21801. https://doi.org/10.1029/2007GL031032

Arlander, D. W., Cronn, D. R., Farmer, J. C., Menzia, F. A., & Westberg, H. H. (1990). Gaseous oxygenated hydrocarbons in the remote marine troposphere. *Journal of Geophysical Research*, *95*(D10), 16,391–16,403. https://doi.org/10.1029/JD095iD10p16391

Arnold, S. R., Spracklen, D. V., Williams, J., Yassaa, N., Sciare, J., Bonsang, B., et al. (2009). Evaluation of the global oceanic isoprene source and its impacts on marine organic carbon aerosol. *Atmospheric Chemistry and Physics*, *9*(4), 1253–1262. https://doi.org/10.5194/acp-9-1253-2009

Baboukas, E. D., Kanakidou, M., & Mihalopoulos, N. (2000). Carboxylic acids in gas and particulate phase above the Atlantic Ocean. *Journal of Geophysical Research*, *105*(D11), 14,459–14,471. https://doi.org/10.1029/1999JD900977

Butkovskaya, N. I., Pouvesle, N., Kukui, A., Mu, Y., & Le Bras, G. (2006). Mechanism of the OH-initiated oxidation of hydroxyacetone over the temperature range 236–298 K. *The Journal of Physical Chemistry. A*, *110*(21), 6833–6843. https://doi.org/10.1021/jp056345r

Calvert, J. G., & Stockwell, W. R. (1983). Acid generation in the troposphere by gas phase chemistry. *Environmental Science and Technology*, *17*, 428–443.

Carlton, A. G., Turpin, H.-J. L., Altieri, K. E., & Seitzinger, S. (2006). Link between isoprene and secondary organic aerosol (SOA): Pyruvic acid oxidation yields low volatility organic acids in clouds. *Geophysical Research Letters*, *33*, L06822. https://doi.org/10.1029/2005GL025374

Chebbi, A., & Carlier, P. (1996). Carboxylic acids in the troposphere, occurrence, sources, and sinks: A review. *Atmospheric Environment*, *30*(24), 4233–4249. https://doi.org/10.1016/1352-2310(96)00102-1

Chhantyal-Pun, R., McGillen, M. R., Beames, J. M., Khan, M. A. H., Percival, C. J., Shallcross, D. E., & Orr-Ewing, A. J. (2017). Temperature-dependence of the rates of reaction of trifluoroacetic acid with Criegee intermediate. *Angewandte Chemie International Edition*, *56*(31), 9044–9047. https://doi.org/10.1002/anie.201703700

Chhantyal-Pun, R., Rotavera, B., McGillen, M., Khan, A., Eskola, A., Caravan, R., et al. (2018). Criegee intermediate-carboxylic acid reactions, A potential source for secondary organic aerosols in the atmosphere, Paper Presented at General Assembly 2018, European Geophysical Union, Vienna, 8–13 April.

Clark, J., English, A. M., Hansen, J. C., & Francisco, J. S. (2008). Computational study on the existence of organic peroxy radical-water complexes ($RO_2.H_2O$). *Journal of Physical Chemistry A*, *112*(7), 1587–1595. https://doi.org/10.1021/jp077266d

Collins, W. J., Stevenson, D. S., Johnson, C. E., & Derwent, R. G. (1997). Tropospheric ozone in a global-scale three-dimensional Lagrangian model and its response to NO_x emission controls. *Journal of Atmospheric Chemistry*, *26*(3), 223–274. https://doi.org/10.1023/A:1005836531979

Derwent, R. G., Collins, W. J., Jenkin, M. E., Johnson, C. E., & Stevenson, D. S. (2003). The global distribution of secondary particulate matter in a 3-D Lagrangian chemistry transport model. *Journal of Atmospheric Chemistry*, *44*(1), 57–95. https://doi.org/10.1023/A:1022139814102

Derwent, R. G., Stevenson, D. S., Doherty, R. M., Collins, W. J., & Sanderson, M. G. (2008). How is surface ozone in Europe linked to Asian and North American NO_x emissions? *Atmospheric Environment*, *42*(32), 7412–7422. https://doi.org/10.1016/j.atmosenv.2008.06.037

Enders, G., Dlugi, R., Steinbrecher, R., Clement, B., Daiber, R., Eijk, J. V., et al. (1992). Biosphere/atmosphere interactions: Integrated research in a European coniferous forest ecosystem. *Atmospheric Environment*, *26*(1), 171–189. https://doi.org/10.1016/0960-1686(92)90269-Q

Galloway, J. N., Likens, G. E., Keene, W. C., & Miller, J. M. (1982). The composition of precipitation in remote areas of the world. *Journal of Geophysical Research*, *87*(C11), 8771–8786. https://doi.org/10.1029/JC087iC11p08771

Granier, C., Lamarque, J. F., Mieville, A., Muller, J. F., Olivier, J., Orlando, J., et al. (2005). POET, a database of surface emissions of ozone precursors. Retrieved from http://accent.aero.jussieu.fr/database_table_inventories.php (last accessed on 02 November 2017)

Grosjean, D. (1989). Organic acids in southern California air: Ambient concentrations, mobile source emissions, in situ formation and removal processes. *Environmental Science and Technology*, *23*(12), 1506–1514. https://doi.org/10.1021/es00070a009

Grosjean, D. (1992). Formic acid and acetic acid: Emissions, atmospheric formation and dry deposition at two southern California locations. *Atmospheric Environment*, *26*(18), 3279–3286. https://doi.org/10.1016/0960-1686(92)90343-J

Haase, K. B., Keene, W. C., Pszenny, A. A. P., Mayne, H. R., Talbot, R. W., & Sive, B. C. (2012). Calibration and intercomparison of acetic acid measurements using proton-transfer-reaction mass spectrometry (PTR-MS). *Atmospheric Measurement Techniques*, *5*(11), 2739–2750. https://doi.org/10.5194/amt-5-2739-2012

Harrington, R. F., Gertler, A. W., Grosjean, D., & Amar, P. (1993). Formic acid and acetic acid in the western sierra Nevada, California. *Atmospheric Environment*, *27*(12), 1843–1849. https://doi.org/10.1016/0960-1686(93)90289-B

Helas, G., Bingemer, H., & Andreae, M. O. (1992). Organic acids over equatorial Africa: Results from DECAFE88. *Journal of Geophysical Research*, *97*(D6), 6187–6193. https://doi.org/10.1029/91JD01438

Hodzic, A., Kasibhatla, P. S., Jo, D. S., Cappa, C. D., Jimenez, J. L., Madronich, S., & Park, R. J. (2016). Rethinking the global secondary organic aerosol (SOA) budget: Stronger production, faster removal, shorter lifetime. *Atmospheric Chemistry and Physics*, *16*(12), 7917–7941. https://doi.org/10.5194/acp-16-7917-2016

Hodzic, A., Madronich, S., Kasibhatla, P. S., Tyndall, G., Aumont, B., Jimenez, J. L., et al. (2015). Organic photolysis reactions in tropospheric aerosols: Effect on secondary organic aerosol formation and lifetime. *Atmospheric Chemistry and Physics*, *15*(16), 9253–9269. https://doi.org/10.5194/acp-15-9253-2015

Ito, A., Sillman, S., & Penner, J. E. (2007). Effects of additional nonmethane volatile organic compounds, organic nitrates, and direct emissions of oxygenated organic species on global tropospheric chemistry. *Journal of Geophysical Research*, *112*, D06309. https://doi.org/10.1029/2005JD006556

Jacob, D. J., & Wofsy, S. C. (1988). Photochemistry of biogenic emissions over the Amazon forest. *Journal of Geophysical Research*, *93*(D2), 1477–1486. https://doi.org/10.1029/JD093iD02p01477

Jenkin, M. E., Watson, L. A., Utembe, S. R., & Shallcross, D. E. (2008). A Common Representative Intermediate (CRI) mechanism for VOC degradation. Part—1: Gas phase mechanism development. *Atmospheric Environment*, *42*(31), 7185–7195. https://doi.org/10.1016/j.atmosenv.2008.07.028

Johns, T. C., Carnell, R. E., Crossley, J. F., Gregory, J. M., Mitchell, J. F. B., Senior, C. A., et al. (1997). The second Hadley Centre coupled ocean-atmosphere GCM: Model description, spinup and validation. *Climate Dynamics*, *13*(2), 103–134. https://doi.org/10.1007/s003820050155

Kanno, N., Tonokura, K., & Koshi, M. (2006). Equilibrium constant of the HO_2-H_2O complex formation and kinetics of $HO_2 + HO_2$-H_2O: Implications for tropospheric chemistry. *Journal of Geophysical Research*, *111*, D20312. https://doi.org/10.1029/2005JD006805

Kawamura, K., Ng, L. L., & Kaplan, I. R. (1985). Determination of organic acids (C_1-C_{10}) in the atmosphere, motor exhaust and engine oils. *Environmental Science and Technology*, *19*(11), 1082–1086. https://doi.org/10.1021/es00141a010

Keene, W. C., & Galloway, J. N. (1986). Considerations regarding sources for formic and acetic acids in the troposphere. *Journal of Geophysical Research*, *91*(D13), 14,466–14,474. https://doi.org/10.1029/JD091iD13p14466

Keene, W. C., Galloway, J. N., Likens, G. E., Deviney, F. A., Mikkelsen, K. N., Moody, J. L., & Maben, J. R. (2015). Atmospheric wet deposition in remote regions: Benchmarks for environmental change. *Journal of the Atmospheric Sciences*, *72*, 2947–2978.

Keene, W. C., Mosher, B. W., Jacob, D. J., Munger, J. W., Talbot, R. W., Artz, R. S., et al. (1995). Carboxylic acids in clouds at a high-elevation forested site in Central Virginia. *Journal of Geophysical Research*, *100*(D5), 9345–9357. https://doi.org/10.1029/94JD01247

Khan, M. A. H., Cooke, M. C., Utembe, S. R., Archibald, A. T., Derwent, R. G., Jenkin, M. E., et al. (2017). Global budget and distribution of peroxyacetyl nitrate (PAN) for present and preindustrial scenarios. *International Journal of Earth & Environmental Sciences*, *2*, 130.

Khan, M. A. H., Cooke, M. C., Utembe, S. R., Archibald, A. T., Derwent, R. G., Jenkin, M. E., et al. (2015). Global analysis of peroxy radicals and peroxy radical-water complexation using the STOCHEM-CRI global chemistry and transport model. *Atmospheric Environment*, *106*, 278–287.

Khan, M. A. H., Cooke, M. C., Utembe, S. R., Archibald, A. T., Maxwell, P., Morris, W. C., et al. (2015). A study of global atmospheric budget and distribution of acetone using global atmospheric model STOCHEM CRI. *Atmospheric Environment*, *112*, 269–277. https://doi.org/10.1016/j.atmosenv.2015.04.056

Khan, M. A. H., Cooke, M. C., Utembe, S. R., Xiao, P., Derwent, R. G., Jenkin, M. E., et al. (2014). Reassessing the photochemical production of methanol from peroxy radical self and cross reactions using the STOCHEM-CRI global chemistry and transport model. *Atmospheric Environment*, *99*, 77–84.

Khan, M. A. H., Jenkin, M. E., Foulds, A., Derwent, R. G., Percival, C. J., & Shallcross, D. E. (2017). A modeling study of secondary organic aerosol formation from sesquiterpenes using the STOCHEM global chemistry and transport model. *Journal of Geophysical Research: Atmospheres*, *122*, 4426–4439. https://doi.org/10.1002/2016JD026415

Khan, M. A. H., Morris, W. C., Galloway, M., Shallcross, B. M. A., Percival, C. J., & Shallcross, D. E. (2017). An estimation of the levels of stabilized Criegee intermediates in the UK urban and rural atmosphere using the steady-state approximation and the potential effects of these intermediates on tropospheric oxidation cycles. *International Journal of Chemical Kinetics*, *49*(8), 611–621. https://doi.org/10.1002/kin.21101

Khan, M. A. H., Percival, C. J., Caravan, R. L., Taatjes, C. A., & Shallcross, D. E. (2018). Criegee intermediates and their impacts on the troposphere. *Environmental Science: Processes & Impacts*, *20*(3), 437–453. https://doi.org/10.1039/c7em00585g

Khare, P., Kumar, N., Kumari, K. M., & Srivastava, S. S. (1999). Atmospheric formic and acetic acids: An overview. *Reviews of Geophysics*, *37*, 227–248.

Khwaja, H. A. (1995). Atmospheric concentrations of carboxylic acids and related compounds at a semi urban site. *Atmospheric Environment*, *29*(1), 127–139. https://doi.org/10.1016/1352-2310(94)00211-3

Kumar, N., Kulshrestha, U. C., Khare, P., Saxena, A., Kumari, K. M., & Srivastava, S. S. (1996). Measurements of formic and acetic acid levels in the vapour phase at Dayalbagh, Agra, India. *Atmospheric Environment*, *30*(20), 3545–3550. https://doi.org/10.1016/1352-2310(96)00042-8

Lim, H. -J., Carlton, A. G., & Turpin, B. J. (2005). Isoprene forms secondary organic aerosol through cloud processing: Model simulations. *Environmental Science and Technology*, *39*(12), 4441–4446. https://doi.org/10.1021/es048039h

Madronich, S., & Calvert, J. G. (1990). Permutation reactions of organic peroxy radicals in the troposphere. *Journal of Geophysical Research*, *95*(D5), 5697–5717. https://doi.org/10.1029/JD095iD05p05697

Malecha, K. T., & Nizkorodov, S. A. (2016). Photodegradation of secondary organic aerosol particles as a source of small, oxygenated volatile organic compounds. *Environmental Science and Technology*, *50*(18), 9990–9997. https://doi.org/10.1021/acs.est.6b02313

McGillen, M. R., Curchod, B. F. E., Chhantyal-Pun, R., Beames, J. M., Watson, N., Khan, M. A. H., et al. (2017). Criegee intermediate-alcohol reactions, a potential source of functionalized hydroperoxides in the atmosphere. *ACS Earth and Space Chemistry*, *1*(10), 664–672. https://doi.org/10.1021/acsearthspacechem.7b00108

Millet, D. B., Guenther, A., Siegel, D. A., Nelson, N. B., Singh, H. B., de Gouw, J. A., et al. (2010). Global atmospheric budget of acetaldehyde: 3-D model analysis and constraints from in-situ and satellite observations. *Atmospheric Chemistry and Physics*, *10*(7), 3405–3425. https://doi.org/10.5194/acp-10-3405-2010

Molina, M. J., Ivanov, A. V., Trakhtenberg, S., & Molina, L. T. (2004). Atmospheric evolution of organic aerosol. *Geophysical Research Letters*, *31*, L22104. https://doi.org/10.1029/2004GL020910

Norton, R. B. (1992). Measurements of gas phase formic and acetic acids at the Mauna Loa Observatory, Hawaii during the Mauna Loa Observatory Photochemistry Experiment 1988. *Journal of Geophysical Research*, *97*(D10), 10,389–10,393. https://doi.org/10.1029/91JD02297

Olivier J. G., Bouwman A. F., Berdowski, J. J., Veldt, C., Bloos, J. P., Visschedijk, A. J., et al. (1996) Description of EDGAR Version 2.0: A set of global emission inventories of greenhouse gases and ozone-depleting substances for all anthropogenic and most natural sources on a per country basis and on 1 degree × 1 degree grid. Technical report, Netherlands Environmental Assessment Agency.

Pan, X., Underwood, J. S., Xing, J. -H., Mang, S. A., & Nizkorodov, S. A. (2009). Photodegradation of secondary organic aerosol generated from limonene oxidation by ozone studied with chemical ionization mass spectrometry. *Atmospheric Chemistry and Physics*, *9*(12), 3851–3865. https://doi.org/10.5194/acp-9-3851-2009

Paulot, F., Wunch, D., Crounse, J. D., Toon, G. C., Millet, D. B., DeCarlo, P. F., et al. (2011). Importance of secondary sources in the atmospheric budgets of formic and acetic acids. *Atmospheric Chemistry and Physics*, *11*(5), 1989–2013. https://doi.org/10.5194/acp-11-1989-2011

Penner, J. E., Atherton, C.S., Dignon, J., Ghan, S. J., Walton, J. J. & Hameed, S. (1994). Global emissions and models of photochemically active compounds. In R. G. Prinn (Ed.), *Global atmospheric biospheric chemistry, Technical Report 223247*. Plenum, New York.

Preunkert, S., Legrand, M., Jourdain, B., & Dombrowski-Etchevers, I. (2007). Acidic gases (HCOOH, CH_3COOH, HNO_3, HCl, and SO_2) and related aerosol species at a high mountain Alpine site (4360 m elevation) in Europe. *Journal of Geophysical Research*, *112*, D23S12. https://doi.org/10.1029/2006JD008225

Puxbaum, H., Rosenberg, C., Gregory, M., Lanzerstorfer, C., Ober, E., & Winiwarter, W. (1988). Atmospheric concentrations of formic and acetic acid and related compounds in eastern and northern Austria. *Atmospheric Environment*, *22*(12), 2841–2850. https://doi.org/10.1016/0004-6981(88)90450-7

Quesada, J., Grossmann, D., Fernández, E., Romero, J., Sanhueza, E., Moortgat, G., & Crutzen, P. J. (2001). Ground based gas phase measurements in Surinam during the LBA-Claire 98 Experiment. *Journal of Atmospheric Chemistry*, *39*(1), 15–36. https://doi.org/10.1023/A:1010762209008

Rosado-Reyes, C. M., & Francisco, J. S. (2006). Atmospheric oxidation pathways of acetic acid. *Journal of Physical Chemistry A*, *110*(13), 4419–4433. https://doi.org/10.1021/jp0567974

Sander, R. (2015). Compilation of Henry's law constants (version 4.0) for water as solvent. *Atmospheric Chemistry and Physics*, *15*, 4399–4981.

Sanhueza, E., & Andreae, M. O. (1991). Emission of formic and acetic acids from tropical Savanna soils. *Geophysical Research Letters*, *18*(9), 1707–1710. https://doi.org/10.1029/91GL01565

Sanhueza, E., Figueroa, L., & Santana, M. (1996). Atmospheric formic and acetic acids in Venezuela. *Atmospheric Environment*, *30*(10-11), 1861–1873. https://doi.org/10.1016/1352-2310(95)00383-5

Sareen, N., Moussa, S. G., & McNeill, V. F. (2013). Photochemical aging of light-absorbing secondary organic aerosol material. *Journal of Physical Chemistry A*, *117*(14), 2987–2996. https://doi.org/10.1021/jp309413j

Schäfer, L., Kesselmeier, J., & Helas, G. (1992). Formic and acetic acid emission from conifers measured with a "cuvette" technique. In S. Beilke, J. Slanina, & G. Angeletti (Eds.), *Field measurements and interpretation of species related to photooxidants and acid deposition, CEC air pollution research* (Vol. 39, pp. 319–323). Brussels: E. Guyot SA.

Schultz Tokos, J. J., Tanaka, S., Morikami, T., Shigetani, H., & Hashimoto, Y. (1992). Gaseous formic and acetic acids in the atmosphere of Yokohama, Japan. *Journal of Atmospheric Chemistry*, *14*(1-4), 85–94. https://doi.org/10.1007/BF00115225

Seco, R., Penuelas, J., & Filella, I. (2007). Short-chain oxygenated VOCs: Emission and uptake by plants and atmospheric sources, sinks and concentrations. *Atmospheric Environment*, *41*(12), 2477–2499. https://doi.org/10.1016/j.atmosenv.2006.11.029

Sindelarova, K., Granier, C., Bouarar, I., Guenther, A., Tilmes, S., Stavrakou, T., et al. (2014). Global data set of biogenic VOC emissions calculated by the MEGAN model over the last 30 years. *Atmospheric Chemistry and Physics*, *14*(17), 9317–9341. https://doi.org/10.5194/acp-14-9317-2014

Singh, H., Chen, Y., Tabazadeh, A., Fukui, Y., Bey, I., Yantosca, R., et al. (2000). Distribution and fate of selected oxygenated organic species in the troposphere and lower stratosphere over the Atlantic. *Journal of Geophysical Research*, *105*(D3), 3795–3805. https://doi.org/10.1029/1999JD900779

Talbot, R. W., Andreae, M. O., Berresheim, H., Jacob, D. J., & Beecher, K. M. (1990). Sources and sinks of formic, acetic, and pyruvic acids over central Amazonia. 2. Wet season. *Journal of Geophysical Research*, *95*(D10), 16,799–16,811. https://doi.org/10.1029/JD095iD10p16799

Talbot, R. W., Beecher, K. M., Harris, R. C., & Cofer, W. R. III (1988). Atmospheric geochemistry of formic and acetic acids at a mid-latitude temperate site. *Journal of Geophysical Research*, *93*(D2), 1638–1652. https://doi.org/10.1029/JD093iD02p01638

Talbot, R. W., Mosher, B. W., Heikes, B. G., Jacob, D. J., Munger, J. W., Daube, B. C., et al. (1995). Carboxylic acids in the rural continental atmosphere over the eastern United States during the Shenandoah Cloud and Photochemistry Experiment. *Journal of Geophysical Research*, *100*(D5), 9335–9343. https://doi.org/10.1029/95JD00507

Utembe, S. R., Watson, L. A., Shallcross, D. E., & Jenkin, M. E. (2009). A Common Representative Intermediates (CRI) mechanism for VOC degradation. Part 3: Development of a secondary organic aerosol module. *Atmospheric Environment*, *43*(12), 1982–1990. https://doi.org/10.1016/j.atmosenv.2009.01.008

Vereecken, L., Novelli, A., & Taraborrelli, D. (2017). Unimolecular decay strongly limits the atmospheric impact of Criegee intermediates. *Physical Chemistry Chemical Physics*, *19*(47), 31,599–31,612. https://doi.org/10.1039/C7CP05541B

Vet, R., Artz, R. S., Carou, S., Shaw, M., Ro, C. -U., Aas, W., et al. (2014). A global assessment of precipitation chemistry and deposition of sulfur, nitrogen, sea salt, base cations, organic acids, acidity and pH, and phosphorous. *Atmospheric Environment*, *93*, 3–100. https://doi.org/10.1016/j.atmosenv.2013.10.060

von Kuhlmann, R., Lawrence, M. G., Crutzen, P. J., & Rasch, P. J. (2003). A model for studies of tropospheric ozone and nonmethane hydrocarbons: Model evaluation of ozone-related species. *Journal of Geophysical Research*, *108*(D23), 4729. https://doi.org/10.1029/2002JD003348

Watson, L. A., Shallcross, D. E., Utembe, S. R., & Jenkin, M. E. (2008). A Common Representative Intermediate (CRI) mechanism for VOC degradation. Part 2: Gas phase mechanism reduction. *Atmospheric Environment*, *42*(31), 7196–7204. https://doi.org/10.1016/j.atmosenv.2008.07.034

Welz, O., Eskola, A. J., Sheps, L., Rotavera, B., Savee, J. D., Scheer, A. M., et al. (2014). Rate coefficients of C1 and C2 Criegee Intermediate reactions with formic and acetic acid near the collision limit: Direct kinetics measurements and atmospheric implications. *Angewandte Chemie International Edition*, *53*(18), 4547–4550. https://doi.org/10.1002/anie.201400964

Yu, S. (2000). Role of organic acids (formic, acetic, pyruvic and oxalic) in the formation of cloud condensation nuclei (CCN): A review. *Atmospheric Research*, *53*(4), 185–217. https://doi.org/10.1016/S0169-8095(00)00037-5

Zervas, E., Montagne, X., & Lahaye, J. (2001). C_1-C_5 organic acid emissions from an SI engine: Influence of fuel and air/fuel equivalence ratio. *Environmental Science and Technology*, *35*(13), 2746–2751. https://doi.org/10.1021/es000237v

Zhang, Y. L., Lee, X. Q., & Cao, F. (2011). Chemical characteristics and sources of organic acids in precipitation at a semi-urban site in Southwest China. *Atmospheric Environment*, *45*(2), 413–419. https://doi.org/10.1016/j.atmosenv.2010.09.067